RSC Advances

ROYAL SOCIETY OF CHEMISTRY

www.rsc.org/advances

Journal Name

COMMUNICATION

One-pot solvothermal synthesis of S doped BiOCl for solar water oxidation

Received 00th January 20xx,
Accepted 00th January 20xx

DOI: 10.1039/x0xx00000x

www.rsc.org/

Zaiyong Jiang,[a] Yuanyuan Liu,[*a] Tao Jing,[b] Baibiao Huang,[*a] Zeyan Wang,[a] Xiaoyang Zhang,[a] Xiaoyan Qin[a] and Ying Dai[b]

Uniformly dispersed sulfur doped BiOCl was prepared via one-pot solvothermal method, which displays higher photocatalytic activity towards oxygen evolution from water compared to pure BiOCl. This is associated with the impurity states above the valence band induced by S doping, which is beneficial for the separation of photo-generated electron-hole pairs.

Since the discovery of photocatalytic water splitting on TiO_2 electrode by Honda et al in 1972,[1] semiconductor photocatalysis attracted massive research interests due to its potential applications in renewable energy substitutes and environmental decontamination.[2-5] Up to now, many kinds of semiconductor photocatalysts, utilizing the abundant solar energy to degrade organic pollutants or split water, are developed, such as, TiO_2,[6] ZnO,[7] Fe_2O_3,[8] Bi_2WO_6,[9] $BiVO_4$,[10] BiOX(Cl, Br, I),[11] WO_3[12] and Bi_2O_3,[13] etc.

[a]*State Key Lab of Crystal Materials, Shandong University, Jinan, 250100, China. E-mail: yyliu@sdu.edu.cn; bbhuang@sdu.edu.cn.*
[b]*School of Physics, Shandong university, Jinan, 250100, China*
†Electronic supplementary information (ESI) available: Experimental details. See DOI: 10.1039/x0xx00000x

Among them, BiOCl is a nontoxic, inexpensive and environmental friendly photocatalyst. Therefore, BiOCl receives more and more attentions for both scientific interests and practical applications. BiOCl has a layered structure, which consists of a $[Bi_2O_2]^{2+}$ layer and two chlorine layers, which are connected via the internal static electric fields. The internal static electric fields of BiOCl can enhance the separation of photo-generated electron-hole pairs,[11,14] which is a key factor to its high photocatalytic activity. The studies on BiOCl as a p-type semiconductor are mainly focused on degradation of organic compounds.[15,16] However, the O_2 evolution of light-driven water splitting over BiOCl photocatalyst is rarely reported, as far as we know.

Till to now, many strategies are proposed to improve the efficiency of semiconductor photocatalysts, such as, doping, semiconductor composite and crystal-facet control, etc. Among them, doping is one of the most attractive methods for improving the photocatalytic O_2 evolution performance, which was demonstrated by some recent researches, such as Mo-doped $BiVO_4$,[17] W-doped $BiVO_4$[18] and P-doped $BiVO_4$[19]. Therefore, it is ideal to enhance the

photocatalytic O_2 evolution performance from water of BiOCl via doping modification.

Herein, in our work, we prepared sulfur doped BiOCl (BiOCl-S) photocatalyst via one-pot facile solvothermal method, in which S elements were uniformly dispersed on BiOCl. The down spin energy band structures were calculated and three impurity states above the valence band of BiOCl-S could be observed. The two impurity states closest valence band can significantly enhance the electron-hole separation efficiency and slightly widen the light absorption. Consequently, the combined effects lead to enhanced O_2 evolution activity of BiOCl-S under ultraviolet-visible (UV-Vis) light irradiation.

The XRD patterns of pure BiOCl and BiOCl-S are shown in Fig. 1a. All the diffraction peaks for the two samples could be perfectly indexed to the characteristic diffraction of tetragonal phase of BiOCl (JCPDS No. 85-861). It can be observed that the BiOCl-S presents similar peak profiles to that of pure BiOCl, and no extra peaks of Bi_2O_3, BiSCl, or Bi_2S_3 are detected. Therefore, BiOCl-S sample maintains the crystal structure as pure BiOCl. In order to further investigate the structural information of the BiOCl-S, Raman spectra were carried out. For comparison, pure BiOCl and Bi_2S_3 were also investigated and the results were given in Fig. 1b. There are three vibrational peaks at 141, 199 and 397 cm^{-1} for both pure BiOCl and BiOCl-S, which can be regarded as A_{1g} and E_g of Bi-Cl stretching mode and the vibration of Bi-O, respectively.[20,21] The characteristic Raman peaks of Bi_2S_3 (located at 236.7 and 259.8 cm^{-1}) are not found in BiOCl-S. This result indicates that there is no Bi_2S_3 in the BiOCl-S, which is consistent with the XRD results discussed above.

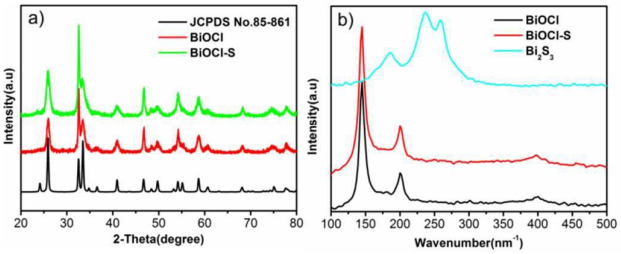

Fig. 1. XRD patterns of BiOCl and BiOCl-S (a), Raman spectra for BiOCl, BiOCl-S and Bi_2S_3 (b)

The morphologies of the samples were investigated by scanning electron microscopy (SEM), which were shown in Fig. 2a and 2b. It can be seen that both samples possess a sphere-like morphology formed via interlaced nanosheets. No distinct differences are observed between pure BiOCl and BiOCl-S. Therefore, the morphology of BiOCl remains after sulfur doping. Chemical element mapping analysis (Fig. 2c) exhibits that the elements including bismuth, chlorine and sulfur are uniformly distributed within the BiOCl-S sample. This confirms the presence of S elements and its homogeneous dispersion in the BiOCl-S.

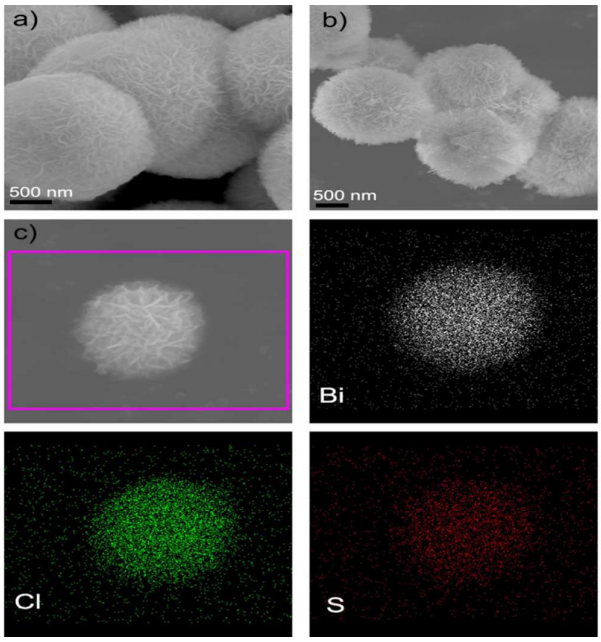

Fig. 2. SEM images of BiOCl (a), BiOCl-S (b) and chemical element mapping data of BiOCl-S (c)

To check the substitution of S for the O site or Cl site of BiOCl, the formation energies of the BiOCl-S with S ions on the O site and Cl site were calculated, and the values are 3.23 eV and 2.76 eV, respectively. The result indicates that S atom is easier to replace the Cl atom compared to the O atom. For BiOCl-S, the calculated lattice parameter is a= 3.910 and c= 7.385, while for a conventional cell the value is a= 3.907 and c= 7.404. The slightly growth of a axis and decrease of c axis can been attributed to the similar ion radius between S^{2-} (0.184nm) and Cl^{-} (0.181nm).

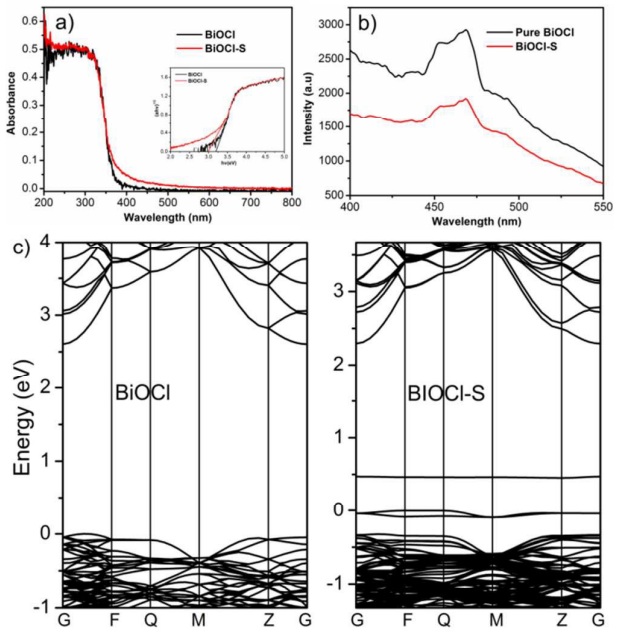

Fig. 3. UV-Visible DRS spectra (a), PL spectra (b) and calculated down spin energy band structures of BiOCl and BiOCl-S (c), (inset of a) plots of $(ahv)^{1/2}$ versus the photon energy (hv).

Fig. 3a presents the UV-Visible diffuse reflection spectra (DRS) spectra of the as-prepared samples. Compared to the pure BiOCl sample, the absorption onset of BiOCl-S is slightly red shifted, revealing that S doping changes the BiOCl absorption behavior. Furthermore, the band gap of BiOCl-S (inset of Fig. 3a) is determined to be 3.0 eV, 0.2 eV lower than that of pure BiOCl (3.2 eV).

The down spin energy band structures for pure BiOCl and BiOCl-S were calculated and presented in Fig. 3c. As can be seen, the band gap is not significantly changed after S doping. However, for BiOCl-S, three impurity states appear in the band gap with two occupied states near Fermi level while the other unoccupied state above it. The two impurity states near Fermi level facilitate the electron-hole separation. Furthermore, the impurity states are responsible for the smaller band gap of BiOCl-S.

Photoluminescence (PL) spectra were applied to test the recombination rate of photogenerated electrons and holes, and the results were shown in Fig. 3b. As can be seen, the main emission for both pure BiOCl and BiOCl-S locates at about 468 nm. However, the emission intensity of BiOCl-S decreases compared to that of pure BiOCl, suggesting a much lower recombination rate of photo-generated charge carriers for BiOCl-S than that for pure BiOCl.[22] In other words, the slower recombination rate over BiOCl-S means the photogenerated electrons and holes in the BiOCl-S could be better separated than those in the pure BiOCl because the introduction of S element has immensely suppressed the recombination of photo-generated charge carriers. This result suggests that BiOCl-S may show a good photocatalytic performance.

Fig. 4a shows the photocatalytic water oxidation activity of BiOCl-S, which was carried out in 100 mL of aqueous $AgNO_3$ solution under UV-Vis light irradiation.

Here, $AgNO_3$ is used as a sacrificial reagent. For comparison, the photocatalytic activity of pure BiOCl was also investigated under the same conditions. It is observed that BiOCl-S exhibits much higher O_2 evolution rate than pure BiOCl, about 5 times higher.

In order to find out the enhanced photocatalytic activity of BiOCl-S, the band decomposed charge-density were calculated and shown in Fig. 4b. It is found that the occupied impurity states are mainly composed of O atoms in Bi_2O_2 layer, S atom, and Cl atoms, and the delocalized nature of the impurity states means the holes possess a large mobility, which is conducive to the carriers transferring to the surface of semiconductor to improve the photocatalytic O_2 evolution activity.

Based on both the theoretical and experimental results, two reasons are proposed to explain the higher photocatalytic activity of BiOCl-S. The first maybe due to the fact that BiOCl-S reduces the band gap to slightly widen the light absorption than pure BiOCl. The second reason is that S doping provides two impurity states above the valence band, which is beneficial for the separation of the photo-generated electrons and holes to enhance photocatalytic performance.

Furthermore, the possible photocatalytic mechanism for photocatlytic O_2 evolution over the BiOCl-S photocatalyst was proposed in Fig. 4c. Upon UV-Vis light irradiation, BiOCl-S absorbs a photon, and the electron is transferred to the conductor band (CB), leaving a hole in the impurity state band. The photo-generated electrons on CB can react with Ag^+ in the $AgNO_3$ aqueous solution, which is used as electrons acceptor to reduce the recombination of electron-hole pairs. On the other hand, the photo-generated holes on VB directly oxides water giving rise to O_2.

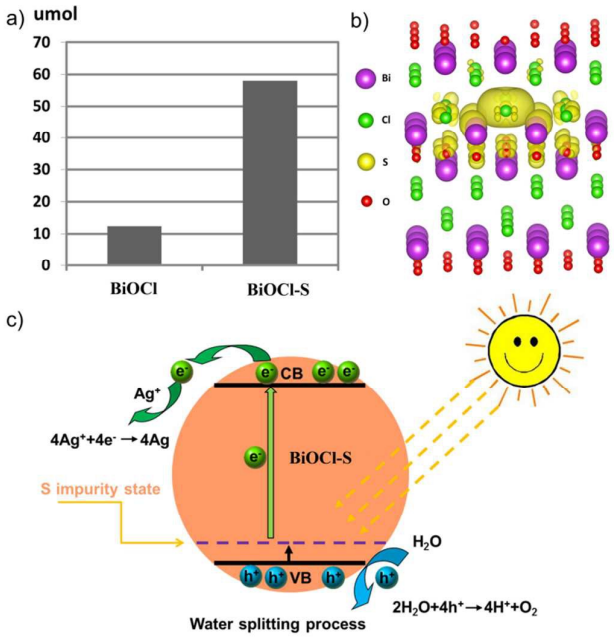

Fig. 4 Photocatalytic O_2 evolution of pure BiOCl and BiOCl-S under UV-Visible light irradiation (a), the calculated band decomposed charge-density for BiOCl-S (b) and schematic illustration of the photocatalytic process of BiOCl-S (c)

In summary, a novel BiOCl-S photocatalyst was synthesized via one pot ion liquid-assisted solvothermal method, in which S elements are uniformly dispersed into the BiOCl without forming any segregated impurity phase. The BiOCl-S photocatalyst displays enhanced photocatalytic O_2 evolution activity compared to pure BiOCl under UV-Visible light irradiation. The reason could be attributed to S doping, which not only slightly extends the light absorption but also significantly improves the separation efficiency of the photogenerated electron-hole pairs. Engineering a simple one-step method to fabricate the BiOCl-S photocatalyst for O_2 evolution may

open a new avenue to design BiOCl photocatalyst for future applications.

Acknowledgements

This work was financially supported by a research Grant from the National Basic Research Program of China (No. 2013CB632401), the National Natural Science Foundation of China (Nos. 21333006, 11374190, 51002091, 21007031).

Notes and references

1 A. Fujishima, K. Honda, *Nature*., 1972, **238**, 37.

2 C. C. Chen, W. H. Ma, J. C. Zhao, *Chem. Soc. Rev*., 2010, **39,** 4206.

3 S. Das, W. M. A. W. Daud, *RSC Adv.*, 2014, **4**, 20856.

4 A. Kudo, Y. Miseki, *Chem. Soc. Rev*., 2009, **38**, 253.

5 T. Y. Kou, C. H. Jin, C. Zhang, J. Z. Sun, Z. H. Zhang, *RSC Adv.*, 2012, **2**, 12636.

6 M. Y. Wang, J. Loccozia, L. Sun, C. J. Lin, Z. Q. Lin, *Energy Environ. Sci.,* 2014, **7**, 2182.

7 D. Chu, Y. Masuda, T. Ohji, K. Kato, *Langmuir*., 2010, **26**, 2811.

8 H. Xie, Y. Z. Li, S. F. Jin, J. J. Han, X. J. Zhao, *J. Phys. Chem. C.*, 2010, **114**, 9706.

9 H. F. Cheng, B. B. Huang, Y. Y. Liu, Z. Y. Wang, X. Y. Qin, X. Y. Zhang, Y. Dai, *Chem. Commun*., 2012, **48**, 9729.

10 Y. M. Yang, Y. Y. Liu, B. B. Huang, R. Zhang, Y. Dai, X. Y. Qin, X. Y. Zhang, *RSC Adv.*, 2014, **4**, 20058.

11 H. F. Cheng, B. B. Huang, Y. Dai, *Nanoscale*., 2014, **6**, 2009.

12 D. Chen, J. H. Ye, *Adv. Funct. Mater*., 2008, **18,** 1922.

13 J. J. Hu, G. Q. Xu, J. W. Wang, J. Lv, X, Y. Zhang, T. Xie, Z. X. Zheng, Y. C. Wu, *Dalton Trans.,* 2015*,* **44**, 5386.

14 J. Jiang, K. Zhao, X. Y. Xiao, L. Z. Zhang, *J. Am. Chem. Soc*., 2012, **134**, 4473.

15 H. L. Peng, C. K. Chan, S. Meister, X. F. Zhang, Y. Cui, *Chem. Mater*., 2009, **21**, 247.

16 S. X. Weng, B. B. Chen, L. Y. Xie, Z. Y. Zheng, P. Liu, *J. Mater. Chem. A*, 2013, **1**, 3068.

17 W. J. Luo, Z. S. Li, T. Yu, Z. G. Zou, *J. Phys. Chem. C*., 2012, **116**, 5076.

18 W. J. Luo, J. J. Wang, X. Zhao, Z. Y. Zhao, Z. S. Li, Z. G. Zou, *Phys. Chem. Chem. Phys*., 2013, **15**, 1006.

19 W. J. Jo, J. W. Jang, K. J. Kong, H. J. Kang, J. Y. Kim, H. Jun, K. P. S. Parmar, J. S. Lee, *Angew. Chem. Int. Ed*., 2012, **51**, 3147.

20 J. Geng, W. H. Hou, Y. N. Lv, J. J. Zhu, H. Y. Chen, *Inorg. Chem*., 2005, **44**, 8503.

21 K. Zhang, J. Liang, S. Wang, J. Liu, K. X. Ren, X. Zheng, H. Luo, Y. J. Peng, X. Zou, X. Bo, J. H. Li, X. B. Yu, *Cryst. Growth Des*., 2012, **12**, 793.

22 J. Di, J. X. Xia, S. Yin, H. Xu, L. Xu, Y. G. Xu, M. Q. He, H, M. Li, *RSC Adv*., 2014, **4**, 14281.